

A 66-112.5 GHz low noise amplifier with minimum NF of 3.9 dB in 0.1- μ m GaAs pHEMT technology

LI Ze-Kun¹, CHEN Ji-Xin^{1,2*}, ZHENG Si-Dou¹, HONG Wei^{1,2}

(1. State Key Laboratory for Millimeter Waves, Southeast University, Nanjing 210096, China;
2. Purple Mountain Laboratory, Nanjing 211111, China)

Abstract: A wideband low noise amplifier (LNA) covering the whole W-band in 0.1- μ m GaAs pHEMT technology is designed. To reduce the inter-stage crosstalk and obtain wideband matching, a bypass circuit composed of dual shunt capacitors is proposed to provide wideband RF grounding. The wideband input matching and optimal noise matching are implemented by a dual-resonance input matching network. The measurement results exhibit a peak gain of 20.4 dB at 108 GHz. The measured small signal gain is 16.9-20.4 dB across 66-112.5 GHz. The measured noise figure (NF) is 3.9 dB at 90 GHz. The measured input 1-dB compression point (IP_{1dB}) is around -12 dBm in W-band.

Key words: GaAs pHEMT, low noise amplifier (LNA), wide band, W-band

基于 0.1- μ m GaAs pHEMT 工艺的最小噪声系数 3.9 dB 的 66~112.5 GHz 低噪声放大器

李泽坤¹, 陈继新^{1,2*}, 郑司斗¹, 洪 伟^{1,2}

(1. 东南大学 毫米波全国重点实验室, 江苏 南京 210096;
2. 紫金山实验室, 江苏 南京 211111)

摘要: 本文基于 0.1- μ m 砷化镓赅配高电子迁移率晶体管 (GaAs pHEMT) 工艺, 研制了一款覆盖整个 W 波段的宽带低噪声放大器。提出了一种由双并联电容组成的旁路电路, 能够提供宽带射频接地, 减小了级间串扰, 利于实现宽带匹配。采用双谐振匹配网络实现了宽带的输入匹配和最佳噪声匹配。实测结果显示, 最大增益在 108 GHz 处达到 20.4 dB, 在 66~112.5 GHz 范围内, 小信号增益为 16.9~20.4 dB。在 90 GHz 处, 实测噪声系数为 3.9 dB。实测的输入 1-dB 压缩点在整个 W 波段内约为 -12 dBm。

关 键 词: 砷化镓赅配高电子迁移率晶体管; 低噪声放大器; 宽带; W 波段

中图分类号: TN454 文献标识码: A

Introduction

With the development of millimeter-wave (mm-wave) theory and technology, modern testing and measurement instruments should possess higher frequency response and precision to meet the demands of high-frequency signal measurement^[1-4]. The ultra-wideband low noise amplifier (UWB LNA) with the characteristics of wideband, high gain, and low noise, can amplify signals, and improve the accuracy and sensitivity of the

measurement, which can play an important role in testing instruments such as oscilloscopes, spectrum analyzers, and vector network analyzers.

Previous works^[1, 3-8] demonstrated UWB LNA in W-band. However, the bandwidth or the gain flatness is not satisfying in the whole W-band. Due to the low single-stage gain in W-band, cascading multi-stage to achieve appreciable gain is a common solution. In Refs. [1] and [6], four identical stages are cascaded to achieve high gain in W-band. However, the gain flatness is not good

Received date: 2023- 06- 20, revised date: 2023- 10- 22

收稿日期: 2023- 06- 20, 修回日期: 2023- 10- 22

Foundation items: Supported by the National Natural Science Foundation of China (62188102)

Biography: LI Ze-Kun (1996-), male, Quanzhou, PhD. Research area involves millimeter-wave and terahertz integrated circuits and system. E-mail: zk-li@seu.edu.cn

* Corresponding author: E-mail: jxchen@seu.edu.cn

in the whole W-band. In Ref. [7], the amplifier is composed of a three-stage input stage and a balanced two-stage output stage to enhance the gain, but the gain flatness is up to 10 dB. Besides, few works discuss the impact of bypass capacitors in the broadband amplifier design.

In this paper, a four-stage UWB LNA covering the whole W-band is proposed for instrument applications. A bypass circuit composed of dual shunt capacitors is proposed to provide a wideband RF grounding, which can reduce the inter-stage crosstalk across the four stages. A dual-resonance input matching network is designed to implement wideband input matching and noise matching. Besides, the gain of each stage is matched at different frequencies in the frequency band to achieve wideband performance.

1 Circuit design

The proposed UWB LNA is designed with the WIN semiconductor GaAs PP10-20 technology. The schematic of the LNA is shown in Fig. 1. The LNA consists of four common source (CS) stages. The transistor gate width is $2 \times 25 \mu\text{m}$ in all stages. The drain bias voltage V_{dd} and the gate bias voltage V_g are 2 V and -0.3 V, respectively. The total current is 44 mA. The gate bias voltage is fed through a large resistor of 2 k Ω to prevent RF loss. 9- Ω resistors R_1 and R_2 are added to the drain bias path in the second and third stages to improve the stability at low-frequency bands.

The proposed UWB LNA is a single-ended topology. In the inter-stage matching network design of a single-ended amplifier, bypass capacitors are necessary to implement RF ground and reduce the inter-stage crosstalk. In the broadband amplifier design, the key basis is the broadband bypass RF ground. The short circuit is provided by the series resonance formed by the capacitor and the parasitic inductance of the ground back hole, as shown in Fig. 2(a). In general, a single shunt capacitor can provide one resonance, as shown in Fig. 2(b). How-

ever, the bandwidth of the RF isolation is limited when using the single shunt capacitor. In the work, dual shunt capacitors (see Fig. 2(a)) with different capacitances are proposed to provide a wideband RF isolation. As shown in Fig. 2(b), the bypass circuit composed of dual shunt capacitors can provide >30 dB isolation in the whole W-band.

The degeneration inductor is utilized at the first stage to increase the real part of the input impedance, and make the optimum noise and gain impedance closer^[5-6]. The input matching network is designed with dual resonance and provides a good compromise between the noise and gain matching. Terminated at 50- Ω resistor, the optimal noise source impedances and the conjugate values of the input impedances of the LNA at 75-110 GHz after input matching are shown in Fig. 3. The optimal noise source impedances are close to 50 Ω . The input matching network provides the dual resonance to implement the wideband input matching.

The simulated gain of each stage and the whole LNA is shown in Fig. 4. The first stage and the second stage are optimized for noise performance. The third stage and the fourth stage are matched for wideband gain performance. The simulated results show a peak gain of 17.6 dB at 93 GHz and a gain flatness of less than 1.5 dB in the whole W-band.

2 Measurement results

The die photograph of the proposed LNA is shown in Fig. 5. The LNA occupies an area of 1.85 mm² (2.1 mm \times 0.88 mm). The S-parameters are measured via on-wafer probing using a Keysight N5245A vector network analyzer with V-band and W-band extenders. In the large-signal measurement, the input signals are generated by a signal source (Keysight E8257D) with $\times 6$ multiplier module (OML S10MS) and an adjustable attenuator.

The measured and simulated small-signal S-parameters of the LNA are shown in Fig. 6(a). The LNA exhib-

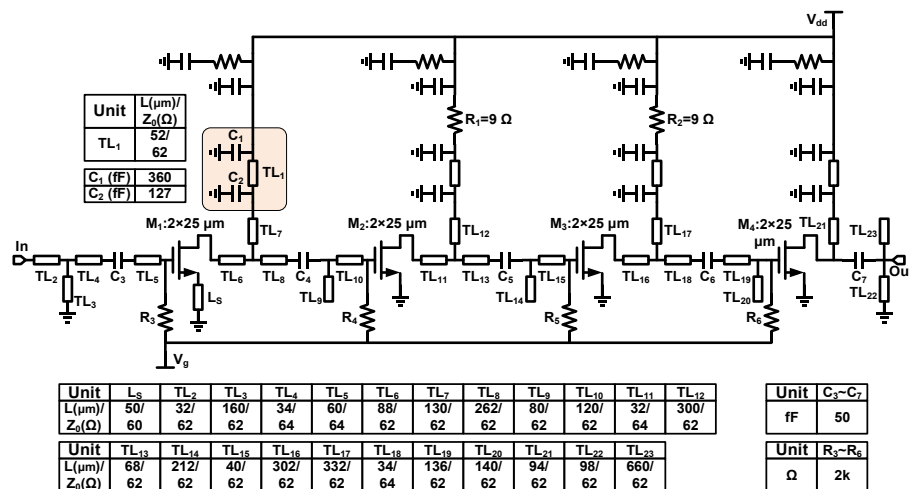


Fig. 1 Schematic of the proposed W-band UWB LNA

图1 W波段超宽带低噪声放大器电路原理图

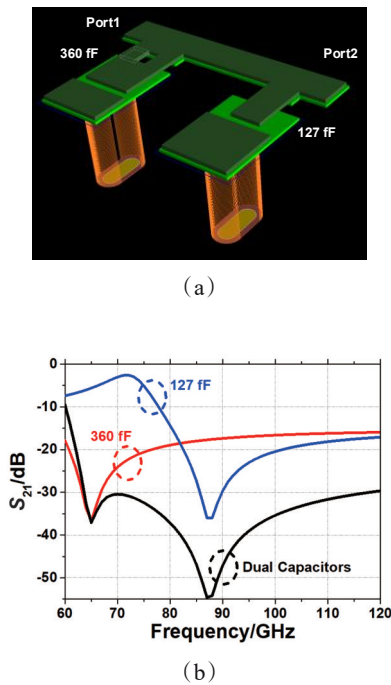


Fig. 2 (a) Layout of dual shunt capacitors; (b) RF isolation of the single shunt capacitor and the dual shunt capacitors

图2 (a)双并联接地电容的版图;(b)单并联接地电容和双并联接地电容的射频隔离度

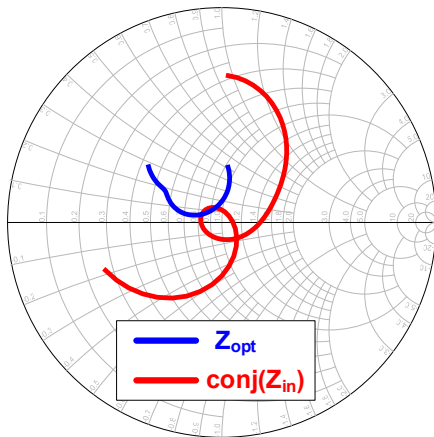


Fig. 3 Optimal noise source impedances and conjugate values of the input impedances of the LNA at 75-110 GHz after input matching

图3 在75~110 GHz频段范围内,经过输入匹配后低噪声放大器的最佳噪声源阻抗值和输入阻抗的共轭值

its a peak gain of 20.4 dB at 108 GHz. The measured small signal gain is 16.9-20.4 dB across 66-112.5 GHz. The stability factor is larger than 1 in the full frequency bands. The measured results show a good agreement with the simulation. The measured gain is slightly higher than the simulation, which might be caused by a shift of the reference plane at the source of the transistor

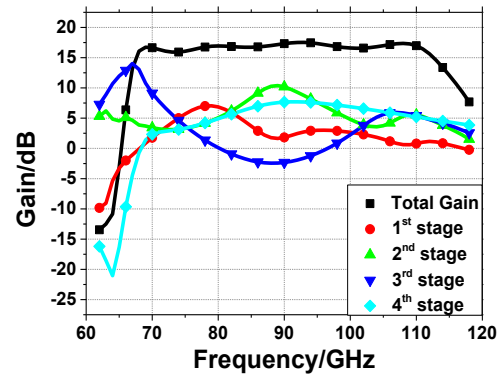


Fig. 4 Simulated gain of the first stage, second stage, third stage, fourth stage and the whole LNA

图4 第一级、第二级、第三级、第四级和整个低噪声放大器的仿真增益

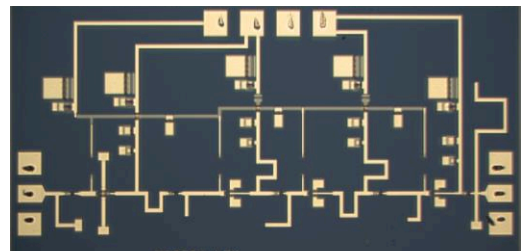


Fig. 5 Die photograph of the proposed LNA

图5 低噪声放大器的芯片显微图

model by a few micrometers.

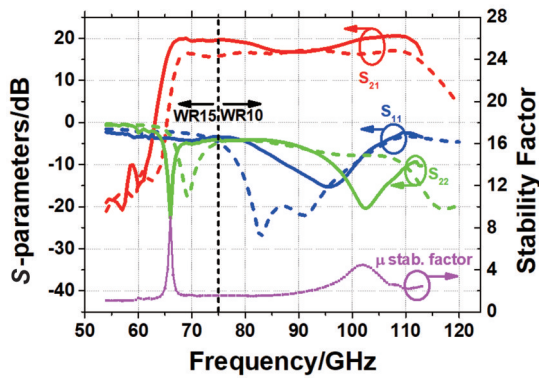
In some broadband applications, the group delay performance of the amplifier in the device needs to be considered. The measured group delay shows variations of ± 15 ps across the whole W-band, as shown in Fig. 6(b).

The measured and simulated input 1-dB compression points (IP_{1dB}) are shown in Fig. 7. The measured IP_{1dB} is around -12 dBm in the whole W-band.

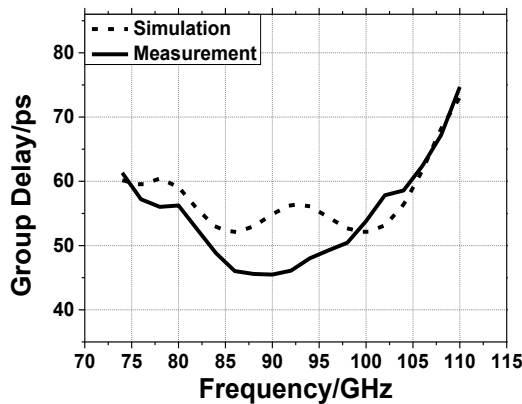
The noise figure (NF) of the LNA is measured by the Y-factor method^[9-10]. The NF measurement setup is shown in Fig. 8. To use the Y-factor method, an excess noise ratio (ENR) source is needed. A W-band mixer module operating at 80-100 GHz with an NF of around 4 dB and a 2-18 GHz LNA module are utilized to convert the RF signals to an intermediate frequency (IF) signal of 2 GHz. The IF signal is fed into the spectrum analyzer to obtain the output noise power density. Turning the noise source on and off, Y can be obtained, which is the difference between the output noise and power density. The ENR is the number given by the noise source. The NF can be calculated by:

$$NF = 10 \times \log_{10} \left(\frac{10^{\frac{ENR}{10}}}{10^{\frac{Y}{10}} - 1} \right) \quad (1)$$

The measured and simulated NFs of the LNA are shown in Fig. 9. The LNA exhibits 3.9 dB NF at 90 GHz. The measured NF is less than 5.1 dB across 75-



(a)



(b)

Fig. 6 (a) Measured (solid lines) and simulated (dashed lines) S -parameters and measured stability factor of the proposed LNA;

(b) measured and simulated group delay of the proposed LNA

图6 (a)实测(实线)和仿真(虚线)的 S 参数以及实测的稳定性系数;(b)实测和仿真的群延时

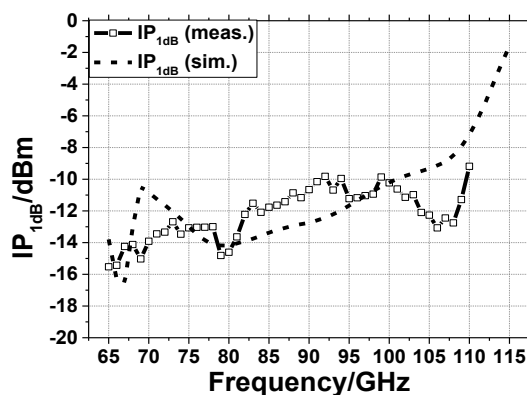


Fig. 7 Measured and simulated input IP_{1dB}

图7 实测和仿真的输入1-dB压缩点

100 GHz.

The performance comparisons with state-of-the-art

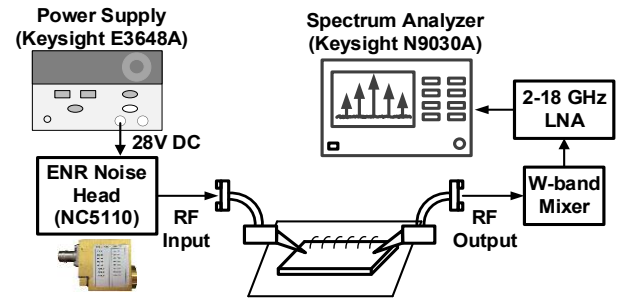


Fig. 8 NF measurement setups of the W-band LNA

图8 W波段低噪声放大器噪声系数测试方案

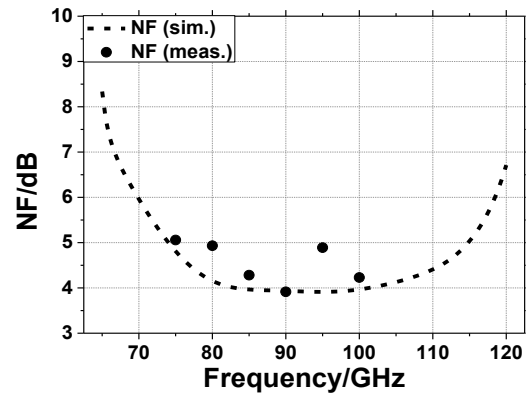


Fig. 9 Measured and simulated NF

图9 实测和仿真的噪声系数

V/W-band LNA in GaAs technologies are summarized in Table 1. The proposed UWB LNA exhibits wide bandwidth covering the whole W-band. The noise and linearity performances are also competitive in W-band LNA.

3 Conclusion

A UWB LNA fabricated by 0.1- μm GaAs pHEMT technology is presented. The dual shunt capacitor bypass circuit and the dual-resonance input matching network are proposed to achieve wideband performance. The UWB LNA exhibits 52.1% percentage bandwidth and the NF is less than 5.1 dB in W-band, which is suitable for instrument applications.

References

- [1] Ciccognani W, Giannini F, Limiti E, *et al.* Full W-band high-gain LNA in mHEMT MMIC technology [C]. 2008 European Microwave Integrated Circuit Conference, IEEE, 2008: 314–317.
- [2] Dyskin A, Ritter D, Kallfass I. Ultra wideband cascaded low noise amplifier implemented in 100-nm GaAs metamorphic-HEMT technology [C]. 2012 International Symposium on Signals, Systems, and Electronics (ISSSE). IEEE, 2012: 1–4.
- [3] Leuther A, Ohlrogge M, Czornomaz L, *et al.* 80 nm InGaAs MOSFET W-band low noise amplifier [C]. 2017 IEEE MTT-S International Microwave Symposium (IMS), IEEE, 2017: 1133–1136.
- [4] Zhang S, Li Q, Zhu W, *et al.* A compact full W-band monolithic low noise amplifier for millimeter-wave imaging [C]. 2018 IEEE International Conference on Integrated Circuits, Technologies and Applications (ICTA), IEEE, 2018: 153–155.
- [5] Li Z, Yan P, Chen J, *et al.* A Wide-Bandwidth W-Band LNA in GaAs 0.1 μm pHEMT Technology [C]. 2020 IEEE MTT-S Interna-

Table 1 Performance comparisons with GaAs-based V/W-band LNA**表 1 基于砷化镓工艺的 V/W 波段低噪声放大器性能对比**

Ref.	Tech.	Freq./GHz	Perc. BW/%	Gain/dB	NF/dB	IP _{1dB} / dBm	P _{DC} /mW	FoM [#]	Area/mm ²
[4]	0.1- μm GaAs pHEMT	75–110	37.8	17–22	4–5*	–20	140	14.7	1.1
[6]	70 nm GaAs mHEMT	75–95	23.5	23–27	2.5–2.7	–	40	203.1	6
[7]	70 nm GaN HEMT	80–122	41.5	24–33.4	3.5–5.5	–7	1840	13.6	3.5
[8]	70 nm GaN HEMT	63–101	46.3	21–24	2.8–3.3	–13	307	24.3	2
[11]	0.1- μm GaAs pHEMT	71–86	19.1	22	4	–11	262.5	5.9	3.75
[12]	0.1- μm GaAs pHEMT	60–77	24.8	28	4.5	–	44	134	2
[13]	0.1- μm GaAs pHEMT	80–94	16.1	12	5	–	72	1.4	1.4
[14]	70 nm GaAs mHEMT	57–66	14.6	23	1.8	–18.8	54	64.7	6
This work	0.1- μm GaAs pHEMT	66–112.5	52.1	16.9–20.4	3.9–5.1	–12	88	26.6	1.85

*Simulated results.

$$\text{FoM} = \frac{S_{21, \text{mag}} \times \text{BW}[\text{GHz}]_{[s]}}{(F - 1) \times P_{\text{DC}}[\text{mW}]}$$

tional Wireless Symposium (IWS), IEEE, 2020: 1–3.

- [6] Ciccognani W, Limiti E, Longhi P E, *et al.* MMIC LNAs for radioastronomy applications using advanced industrial 70 nm metamorphic technology [J]. *IEEE Journal of Solid-State Circuits*, 2010, **45** (10): 2008–2015.
- [7] Thome F, Brückner P, Leone S, *et al.* AW/F-Band Low-Noise Power Amplifier GaN MMIC with 3.5–5.5-dB Noise Figure and 22.8–24.3-dBm Pout [C]. 2022 IEEE/MTT-S International Microwave Symposium-IMS 2022, IEEE, 2022: 603–606.
- [8] Thome F, Brückner P, Leone S, *et al.* A wideband E/W-band low-noise amplifier MMIC in a 70-nm gate-length GaN HEMT technology [J]. *IEEE Transactions on Microwave Theory and Techniques*, 2022, **70**(2): 1367–1376.
- [9] Three Methods of Noise Figure Measurement [R/OL]. <https://www.analog.com/media/en/technical-documentation/tech-articles/noise-figure-measurement-methods-and-formulas--maxim-integrated.pdf>, 2003–11.
- [10] Collantes J M, Pollard R D, Sayed M. Effects of DUT mismatch on the noise figure characterization: a comparative analysis of two Y-factor techniques [J]. *IEEE Transactions on Instrumentation and Measurement*, 2002, **51**(6): 1150–1156.
- [11] Byk E, Couturier A M, Camiade M, *et al.* An E-band very low noise amplifier with variable gain control on 100 nm GaAs pHEMT technology [C]. 2012 7th European Microwave Integrated Circuit Conference, IEEE, 2012: 111–114.
- [12] Lee Y T, Chiong C C, Niu D C, *et al.* A high gain E-band MMIC LNA in GaAs 0.1- μm pHEMT process for radio astronomy applications [C]. 2014 9th European Microwave Integrated Circuit Conference, IEEE, 2014: 456–459.
- [13] Bessemoulin A, Tarazi J, McCulloch M C G, *et al.* 0.1- μm GaAs PHEMT W-band low noise amplifier MMIC using coplanar waveguide technology [C]. 2014 1st Australian Microwave Symposium (AMS), IEEE, 2014: 1–2.
- [14] Longhi P E, Pace L, Colangeli S, *et al.* V-band GaAs metamorphic low-noise amplifier design technique for sharp gain roll-off at lower frequencies [J]. *IEEE Microwave and Wireless Components Letters*, 2020, **30**(6): 601–604.